

Impact velocity and distribution in ultrasonic shot peening

J. Badreddine¹, M. Micoulaut², E. Rouhaud¹, D. Retrait¹, M. Francois¹, S. Remy¹

¹ Laboratoire de Systèmes Mécaniques et d'Ingénierie Simultanée, Université de Technologie de Troyes, UMR CNRS 6279, 12 rue Marie Curie, 10000 Troyes, France

² Laboratoire de Physique Théorique de la Matière Condensée, Université Pierre et Marie Curie, CNRS UMR 7600, Boite 121, 4 place Jussieu, 75252 Paris Cedex 05, France

Abstract

We study the dynamic of shot during an ultrasonic shot peening process from two aspects. The first consists in running various calculations of spheres placed in a cylindrical chamber (radius 35 mm, height 40 mm) and propelled by a sonotrode (frequency 20 kHz, amplitude 25 μm). This allows for a better understanding of the minimal peening time needed to reach a stationary regime. The second aspect deals with the relationship between spatial impact distributions and normal impact velocities. Results show that after a specific peening time, initial conditions such as shot position and velocity have no influence on the calculation output. We also found that the surface impact frequency on a peened sample placed on top of a cylindrical or parallelepiped chamber with same inner volumes does not vary much, and that low velocity impacts are mainly concentrated at the edge of the chamber.

Keywords Ultrasonic shot peening, Shot velocity, Impact distribution, Model

1. Introduction

Ultrasonic shot peening is a mechanical surface treatment process that consists in shooting a sample to be treated (TOP) with spherical shot. The shot are set in the treatment chamber (WALL). A generator produces the vibration of a "sonotrode" (BOT), located in the bottom of the chamber, with a frequency of 20 kHz which propels the shot towards the top with high velocity. The multiple impacts on the part induce compressive residual stresses in the material, thus enhancing its mechanical characteristics as well as its lifetime. These residual stresses highly depend on process parameters such as the shot velocities, the impact angles and the surface coverage [1,2,3,4].

The model presented here simulates the dynamics of hard spheres placed in a rectangular chamber and propelled by a vibrating membrane onto a flat surface, as shown in Figure 1. These spheres represent the shot. An Event-Driven-Dynamics based algorithm [5] allows to follow the trajectory of the spheres. By simulating thousands of impacts onto the treated part, one is able to perform statistical studies for impact velocity and impact angles [6], as well for impact frequency and distribution.

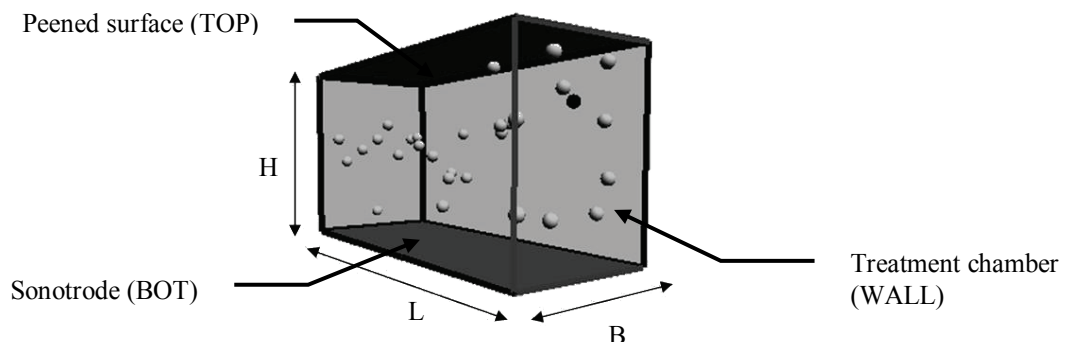


Figure 1: Illustration of the ultrasonic shot peening model for a parallelepipedic chamber

The model detects “shot-shot” and “shot-wall” impacts and takes into account energy dissipation during impact through normal (C_{SHOT} , C_{WALL} , C_{BOT} , C_{TOP}) and tangential (μ) restitution coefficients. The tangential coefficient is considered to be constant with a value of 5/7 [7,8]. The normal coefficients (C_i , $i = [\text{SHOT}, \text{WALL}, \text{BOT}, \text{TOP}]$), on the other hand, follow the power law given below, according to phenomenological models [8] and experiments [9]:

$$C_i(v) = \begin{cases} C_0^i & \text{if } v < v_0^{\text{shot}} \\ C_0^i (v/v_0^{\text{shot}})^{-1/4} & \text{if } v > v_0^{\text{shot}} \end{cases}, \text{ where } v \text{ is the shot velocity} \quad (1)$$

The constant normal restitution coefficients at low velocity will be set as follows: $C_0^{\text{SHOT}} = 0.91$ (100Cr6 Steel shot), $C_0^{\text{BOT}} = 0.91$ (Titanium sonotrode), $C_0^{\text{TOP}} = 0.6$ (Aluminum sample) and $C_0^{\text{WALL}} = 0.6$ (Aluminum chamber). [9,10]

2. Treatment repeatability

Ultrasonic shot peening uses random trajectories of shot during the treatment to achieve homogeneous coverage of impacts/compressive stresses. In this section, we will study the repeatability of peening results and evaluate t_0 , which is defined as the time after which the peening regime is stationary. We will also determine how t_0 evolves with peening parameters. Therefore, we will focus on the effect of the quantity of shot on the impact frequency $F(t)$; the impact frequency being the cumulated amount of impacts as a function of peening time. A cylindrical peening chamber ($R = 35$ mm, $H = 40$ mm) and 3 mm shot will be used for all calculations in section 2.

2.1. Transitory and stationary regimes: t_0

With our model we simulate the peening of a flat surface positioned on top of a cylindrical chamber that contains 30 steel spheres. Six calculations were made using the same peening parameters but with different initial conditions, i.e. initial positions and velocities of the hard spheres that have been randomly placed close to the sonotrode at $t=0$.

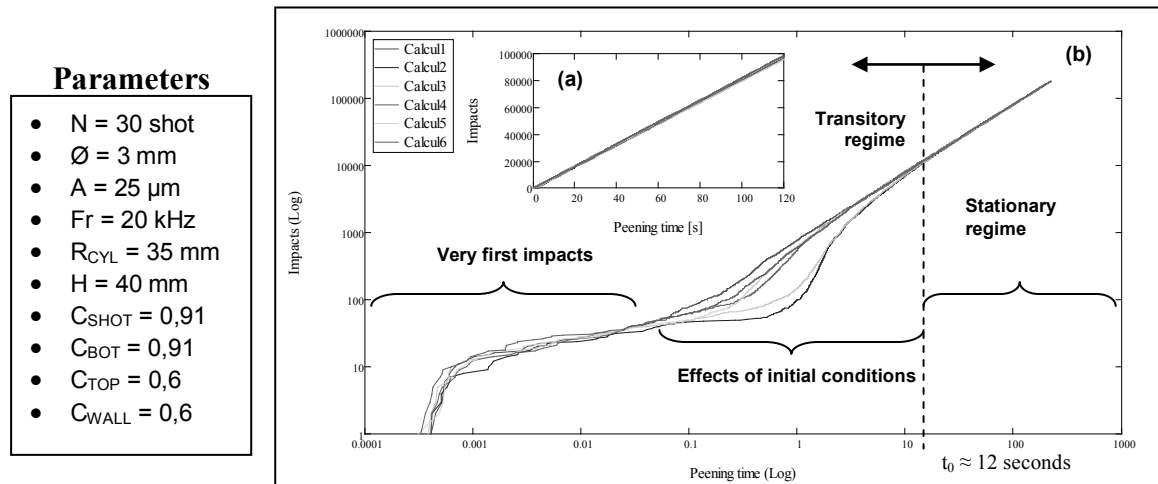


Figure 2: Evolution of impacts on the treated surface as a function of peening time. Six calculations were carried out using the same peening parameters but with different initial shot positions and velocities. **a)** Log-Log plot of the impact frequency $F(t)$. **b)** Linear plot of the impact frequency $F(t)$.

Figure 2 represents the cumulated amount of impacts on the treated surface as a function of peening time. The results from Figure 2(a) show that globally the impact frequency $F(t)$ evolves linearly with peening time. However, in order to distinguish between transitory and stationary regimes, we need to look closer to what happens at very small peening times. To do so, $F(t)$ was plotted in a Log-Log scale (Figure 2(b)), where it is possible to identify

three distinct regimes. The first one contains the very first impacts on the top cover. The second one is the transitory regime where we notice significant differences due to initial conditions. The third one, found at $t > t_0$, correspond to the stationary regime for which it is observed that $F(t)$ increases linearly with peening time (Figure 2(a)).

2.2. Influence of the system density

The quantity t_0 turns out to be system dependent. We therefore focus on the influence of shot quantities on t_0 , by modeling the peening treatment for different amounts of shot. Calculations were run for $N = \{25; 50; 100; 200; 700\}$ hard spheres. It was noticed throughout our studies that above a value of 10,000 impacts on the sample, we were always sure to be in the stationary regime, independently of the system size and parameters. Thus, t_0 will be chosen as the time needed to reach 10,000 impacts on the sample surface.

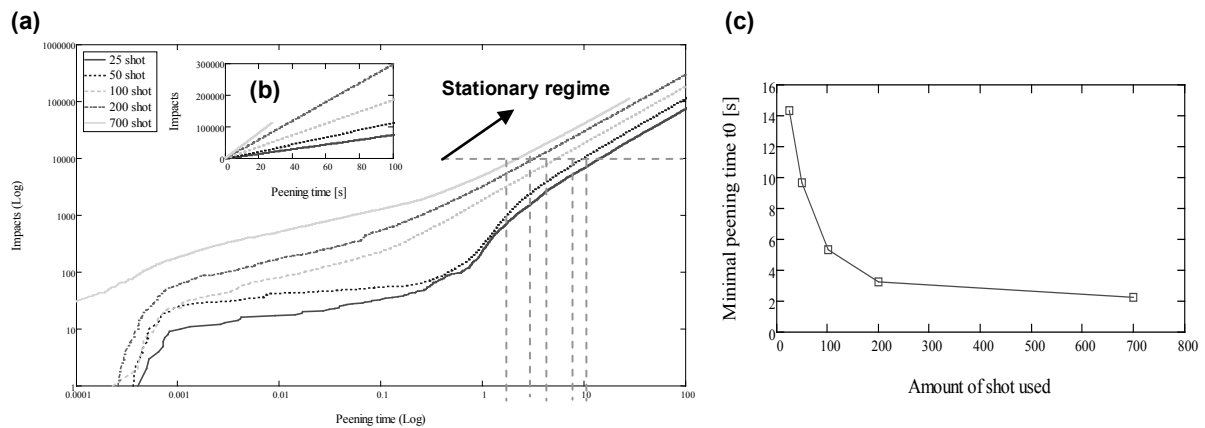


Figure 3: Impact frequency for peened surface treated for at least 30 seconds with different amount of shot: **a)** plotted on a Log-Log scale and **b)** on a linear scale. **c)** Evolution of the minimal peening time t_0 as a function of shot quantity (Linear scale).

In Figure 3(a) we can clearly see both transitory and stationary regimes. More important, a linear evolution (Figure 3(b)) can clearly be observed for each of the five conducted simulations, in the stationary regime. For each curve, t_0 is then extracted and reported in Figure 3(c) as a function of shot quantity. The minimal peening time t_0 decreases rapidly with the increase of the amount of shot used in the chamber. The higher the number of shot in the chamber, the faster the stationary regime is reached, as an increased disorder induced by an increased shot density allows for an earlier loss of the initial conditions. For the following section (§3), all results will be calculated from data beyond the stationary peening time to insure that they do not depend on the initial configuration.

3. Impact coverage

Another way to evaluate the homogeneity of the peening process is to follow a surface coverage rate S_{COV} which is usually very difficult to measure experimentally. However, the latter can be readily computed from the model and informs about peening homogeneity, as we have access to position and time of each impact on the top cover. These data permit indeed to calculate a surface impact frequency [8]. Spatial impact distribution also enables to estimate either a global or local coverage rate by applying a mean size for all impact points.

3.1. Box VS Cylinder

The peening chamber geometry plays an important role in the coverage homogeneity. It has been shown from previous studies that high levels of coverage heterogeneity are usually located near the edges of the treatment chambers [9]. Two chamber geometries with equivalent inner volume and height have been tested: a cylindrical chamber ($R = 35$ mm, $H = 40$ mm) and a box chamber ($L = B = 62$ mm, $H = 40$ mm). The surface impact frequency at the treated samples was calculated in an area of 25 mm in radius, centered in the middle of

both samples. In doing so, we don't include peening irregularities near the edges of the chambers.

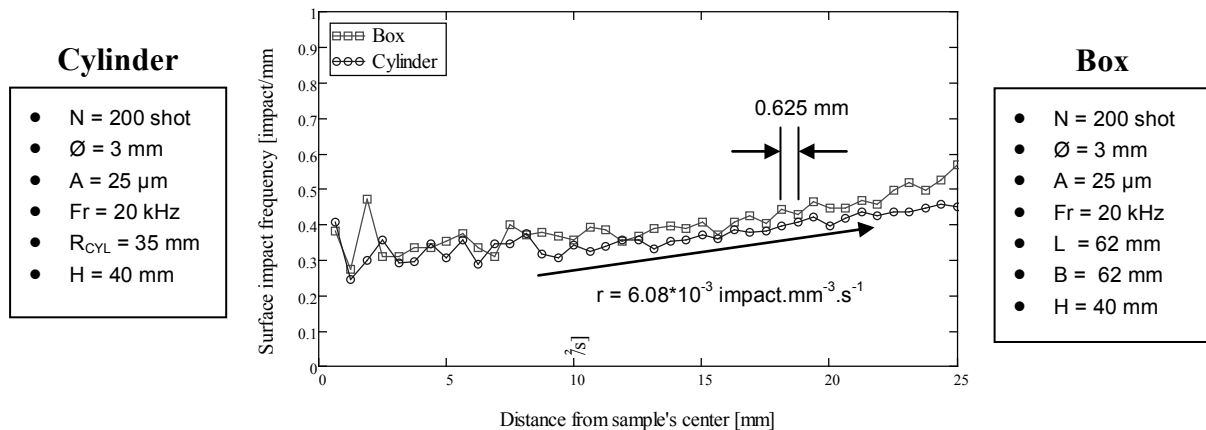


Figure 4: Surface impact frequency along radius for the cylindrical chamber and along both sides for the box chamber. Results were obtained in the stationary regime and for a peening time of 30 seconds. This time corresponds to 89,478 and 62,382 impacts for the Box and Cylindrical chambers respectively.

As illustrated in Figure 4, calculated surface impact frequencies, for both the box and cylindrical geometries, are very similar to each other and seem to increase slightly towards the peening edges of the chamber with a rate of $r = 6.08 \cdot 10^{-3} \text{ impact} \cdot \text{mm}^{-2} \cdot \text{s}^{-1}$ per mm. The surface impact frequency increases from 0.41 to 0.45 $\text{impact} \cdot \text{mm}^{-2} \cdot \text{s}^{-1}$ for the cylindrical chamber, and from 0.38 to 0.57 $\text{impact} \cdot \text{mm}^{-2} \cdot \text{s}^{-1}$ for the box chamber. As a whole, it could be concluded that the geometry of the chamber does not have a major influence on the observed results. This is due to the fact that the shot, in both cases, have an identical free path. This corresponds to the length a shot can travel in the peening chamber without having its trajectories deflected by other shot [11].

3.2. Impact distribution

In § 3.1 we see that a steady surface impact frequency is obtained for both the cylindrical and box chambers. The maximal velocities recorded are respectively 5.33 and 5.41 $\text{m} \cdot \text{s}^{-1}$, the average velocities being respectively 1.56 and 1.40 $\text{m} \cdot \text{s}^{-1}$ for the cylindrical and box geometries. Even though similar global results are obtained for both chambers, normal impact velocities on the impacted samples are far from being evenly distributed across the peened surface.

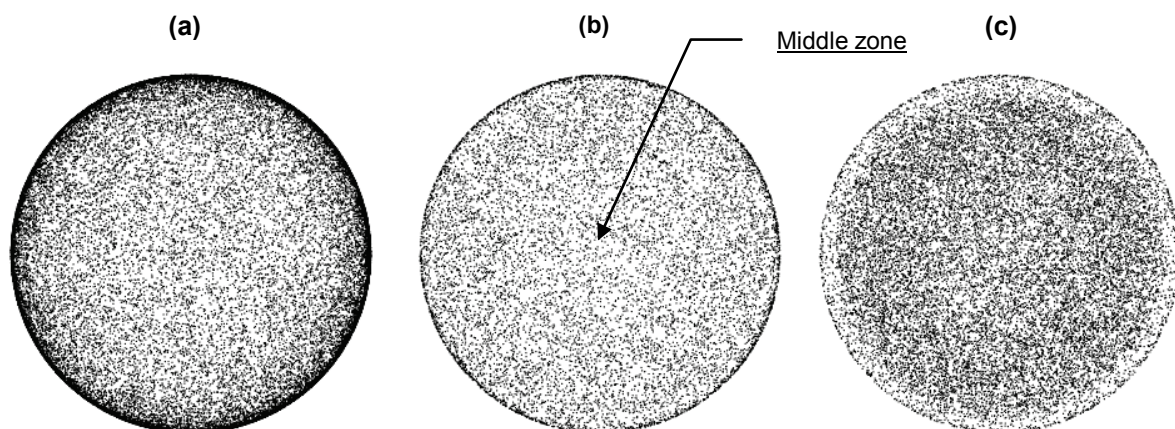


Figure 5: Spatial impact distribution on peened sample for a Cylindrical chamber. **a)** Impacts with a normal velocity lower than 1 $\text{m} \cdot \text{s}^{-1}$. **b)** Impacts with a normal velocity ranging from 1 to 2 $\text{m} \cdot \text{s}^{-1}$. **c)** Impacts with a normal velocity higher than 2 $\text{m} \cdot \text{s}^{-1}$.

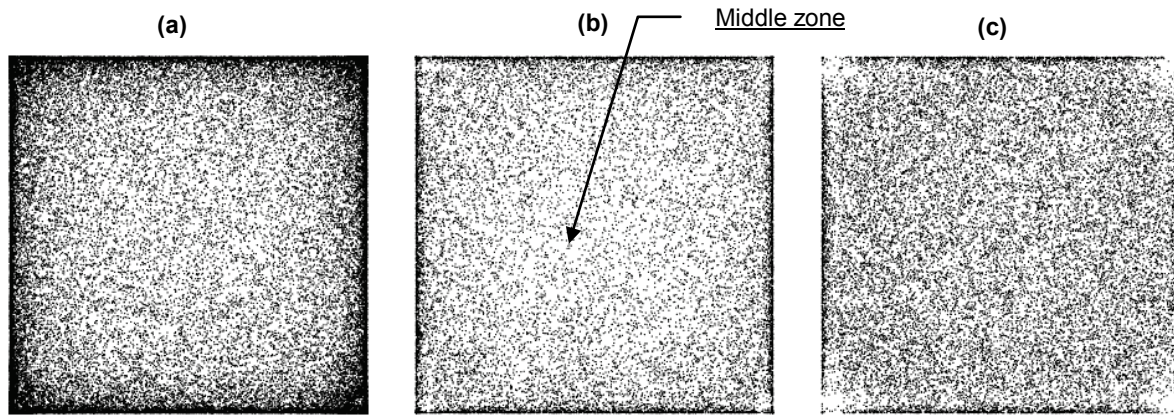


Figure 6: Spatial impact distribution on peened sample for a Box chamber. **a)** Impacts with a normal velocity lower than 1 m.s^{-1} . **b)** Impacts with a normal velocity ranging from 1 to 2 m.s^{-1} . **c)** Impacts with a normal velocity higher than 2 m.s^{-1} .

In Figure 5 and Figure 6, spatial impact distributions on the sample for both the Cylindrical and Box chambers have been separated into three groups. The first group, Figure 5(a) and Figure 6(a), correspond to the impacts with a normal velocity lower than 1 m.s^{-1} . The second group, Figure 5(b) and Figure 6(b), correspond to impacts with a normal velocity ranging from 1 to 2 m.s^{-1} . The last group, Figure 5(c) and Figure 6(c), correspond to the impacts with a normal velocity higher than 2 m.s^{-1} . The average velocities for both geometries are close to 1.5 m.s^{-1} . These results show that the majority of the low impact velocities ($V < 1 \text{ m.s}^{-1}$) is highly concentrated near the edges of the chambers, while the rest of them are scattered in the Middle zone of the sample. On the other hand, impacts with a higher normal velocity ($V > 2 \text{ m.s}^{-1}$) are more gathered in the middle zone of the sample and a little minority of them located at the edges. Impacts with velocities between 1 and 2 m.s^{-1} seem to be more homogeneously distributed across the sample surface, than for the other groups of impacts. These distributions are mainly affected by the inelastic collisions with the walls of the chamber.

Conclusion

Using an event-driven model for hard spheres dynamics, we have shown the existence of a stationary regime for which the influence of the initial conditions (shot positions and velocities) are negligible and the frequency of impact evolves linearly. The time t_0 after which the stationary regime is reached corresponds to an approximate value of $10,000$ impacts on the sample. Results also show that t_0 decreases significantly with the increase of the amount of shot used during the peening process.

Impact distribution across the sample show similar levels of the surface impact frequency for the two chamber geometries. Although results indicate constant levels of surface impact frequency in the studied area (25 mm in radius), the spatial distribution for high and low velocity impacts is different. In fact, the high velocity impacts are mainly located in the middle zone of the sample, whereas the low velocity impacts are mostly located at the edges of the chambers.

Acknowledgement

We wish to express our special thanks to SNECMA, in their support for this research work, which is part of the MAIA project.

References

- [1] H.Y. Miao, S. Larose, C. Perron, M. Lévesque, *On the potential applications of a 3D random finite element model for the simulation of shot peening*, *Advances in Engineering Software* 40 (2009), pp.1023–1038
- [2] Y.M. Xing, J.Lu, *An experimental study of residual stress induced by ultrasonic shot peening*, *Journal of Materials Processing Technology* 152 (2004), pp. 56–61
- [3] Bohdan N. Mordyuk, Georgiy I. Prokopenko, *Ultrasonic impact peening for the surface properties' management*, *Journal of Sound and Vibration* 308 (2007), pp. 855–866
- [4] B.L. Boyce, X. Chen, J.W. Hutchinson, R.O. Ritchie, *The residual stress state due to a spherical hard-body impact*, *Mechanics of Materials* 33 (2001), pp. 441-454
- [5] N. V. Brilliantov, F. Spahn, J.-M. Hertzsch et T. Pöschel, *Model for collisions in granular gases*, *Physical Review* (1996) E 53, 5382
- [6] J. Badreddine, E. Rouhaud, M. Micoulaut, D. Retraint, S. Remy, M. François, P. Viot, G. Doubre-Baboeuf, D. Le Saunier, V. Desfontaine, *Simulation and experimental approach for shot velocity evaluation in ultrasonic shot peening*, *Mécanique & Industries* (Accepted)
- [7] Raymond M. Brach. *Impact dynamics with applications to solid particle erosion*. *Int. J. Impact Engineering* (1998) vol. 7, pp. 37-53
- [8] S. McNamara, E. Falcon. *Simulations of vibrated granular medium with impact-velocity-dependent restitution coefficient*. *Physical Review* (2005) E 71, 031302
- [9] M. Micoulaut, D. Retraint, P. Viot, M. François, *Heterogeneous ultrasonic shot peening : experiment and simulation*, *ICSP9* (2005), Marne la Vallée, France, pp. 119-124
- [10] M. Micoulaut, S. Mechkov, D. Retraint, P. Viot, M. François, *Granular gases in mechanical engineering: on the origin of heterogeneous ultrasonic shot peening*, *Granular Matter* (2007) 9, pp. 25–33
- [11] C. Pilé. *Le grenailage par ultrasons : caractérisation du procédé et influence sur la fatigue d'alliages TiAL*. PhD dissertation (2005), University of Technology of Troyes